

Dynamics of laser-induced molecular alignment in the impulsive and adiabatic regimes: A direct comparison

R. Torres,¹ R. de Nalda,² and J. P. Marangos¹¹*The Blackett Laboratory, Imperial College London, Prince Consort Road, London SW7 2BW, United Kingdom*²*Facultad de Ciencias Químicas, Universidad Complutense de Madrid, Avenida Complutense s/n, 28040 Madrid, Spain*

(Received 12 May 2005; published 30 August 2005)

Quantum-mechanical calculations are performed of the dynamic alignment of linear molecules induced by a strong nonresonant laser field. Within this framework we have treated in a unified fashion the alignment with laser pulses of varying duration from the short pulse impulsive limit ($\tau_{\text{pulse}} \ll T_{\text{rot}}$) to the long pulse adiabatic limit ($\tau_{\text{pulse}} > T_{\text{rot}}$). The temporal behavior of the alignment in both these limits, and in the intermediate pulse duration regime, have been analyzed. For the impulsive limit the dependence of the degree of maximum alignment upon the laser pulse duration was examined and the intensity-dependent optimum pulse duration explained. A comparison between the degree of alignment under the same conditions of pulse intensity and rotational temperature was performed between the impulsive and adiabatic cases. The adiabatic case was found to always provide a better degree of alignment for a given intensity which we show is due to the zero relative phasing between the component states of the superposition that form the pendular states. We have explicitly calculated the angular distribution of an ensemble of linear molecules as it evolves through a rotational revival; a rich structure is found that may be useful in guiding future experiments that utilize the field free alignment in a revival.

DOI: [10.1103/PhysRevA.72.023420](https://doi.org/10.1103/PhysRevA.72.023420)

PACS number(s): 42.50.Vk, 42.50.Hz, 33.80.-b

I. INTRODUCTION

Recent advances in strong field molecular physics have demanded the possibility to acquire control over the orientation of the molecules within the laboratory frame in order to get more insight into the observed phenomena. Particularly, it has been shown both theoretically and experimentally, that the geometry of the molecule and the nature of the highest occupied molecular orbital (HOMO) play an important role in the processes of strong field ionization and high-order harmonic generation (HHG) [1–6]. As a consequence, the harmonic yield is sensitive to the angle between the molecule and the direction of polarization of the laser field [7–12]. This fact has been used recently in order to make a tomographic reconstruction of the HOMO of N₂, allowing a direct observation of a molecular orbital in three dimensions (3D) [13].

Among the various techniques which create a preferred direction in space within a molecular ensemble, those based on a strong nonresonant linearly polarized laser field have been shown to be the most versatile [14–18]. In particular, alignment of both polar and nonpolar molecules is possible because of the high field strengths readily obtained at the focus of a high power pulsed laser. Other methods, such as the so-called “brute force” technique require strong dc electric fields and can only orientate molecules with a large permanent dipole moment [19,20] as alignment of nonpolar molecules requires unfeasibly large dc electric fields.

The use of intense lasers allows the production of electric fields that result in an interaction energy much larger than the rotational energy of the molecules without the technical complications associated with strong static fields. Furthermore, the intense fields of the lasers are readily able to induce second-order effects, i.e., they can produce an induced dipole

moment in the molecules, overcoming the need of a permanent dipole moment [21]. The only requirement is that the molecular polarizability is anisotropic, then the interaction of the molecule with the laser field tends to align the molecules along the direction of maximum polarizability. In linear molecules the polarizability is always anisotropic and the maximum polarizability occurs along the molecular axis.

There are two alternative ways of using a strong laser field to align molecules. If the laser is turned on and off slowly as compared to the rotational period of the molecule, the alignment proceeds adiabatically. The interaction with the external electric field creates a so-called “pendular” state which correlates adiabatically with the field-free rotational eigenstates [14] and, as the laser pulse fades away, the molecular ensemble returns smoothly to the isotropic angular distribution. This technique is termed “adiabatic alignment.”

The other technique employs laser pulses much shorter than the rotational period of the molecule. In this case, the interaction leaves the molecule in a coherent superposition of rotational eigenstates. As noticed by Seideman [22], the generation of a broad wave packet in angular momentum space is a necessary but not sufficient condition to attain molecular alignment. To have a significant degree of order in angular space, the different components of the wave packet must keep a particular phase relation. A rotational wave packet freely evolving in time suffers a periodic dephasing and rephasing of its components, thus the aligned state only lasts for a short while, but it is periodically reconstructed at multiple revival times which persist for a long time after the interaction, until the collisions with other molecules break the quantum coherence [23,24]. This technique is known as “impulsive alignment” because the interaction with the short laser pulse can be viewed as a “kick” imparted to the molecule.

Both methods have advantages and drawbacks which must be considered depending on the application of the aligned molecules. The adiabatic technique requires temporally smooth pulses of ns to ~ 100 ps duration. Generally it provides a high degree of alignment during the laser pulse, and makes multi-axis alignment relatively easy to implement by the use of elliptically polarized fields, however, the presence of the aligning field can critically disturb the strong field processes which are the subject of investigation in most cases. The impulsive method has the advantage of generating field-free aligned molecules, and the process is not sensitive to the details of the pulse shape; furthermore, it presents some peculiarities such as rapidly varying angular distributions that can be utilized for short pulse compression [25,26]. Field-free alignment in 3D can be obtained by a recently proposed method which utilizes two orthogonally polarized time-separated laser pulses [27].

There is also a third technique, initially proposed by Yan *et al.* [28] which can be considered as a hybrid of the two previous methods. In this technique, the field is adiabatically switched on, creating the molecular pendular states, and suddenly turned off. Then the pendular states are allowed to dephase and rephase showing the same revival structure as in the purely impulsive case. In this case the maximum degree of alignment attained at each revival time equals that of the adiabatically prepared system.

Much effort has been given to fully understand the characteristics of both the adiabatic and impulsive alignment and its dynamics [14,17,22–24,29,30], and experimental realization of both techniques have shed light on the processes involved, highlighting new features [26,30–33]. The optimization of the degree of alignment in the impulsive technique has recently been considered. Rosca-Pruna *et al.* [29] performed quantum-mechanical calculations in order to assess the importance of several experimental parameters such as the intensity and pulse duration of the pump pulse and the rotational temperature of the molecular sample. The use of a sequence of pump pulses has also been proposed as a method of increasing the maximum degree of alignment obtained in the laser-molecule interaction, and it has been found that the field free molecular alignment can be significantly improved by the use of a proper train of strong ultrashort laser pulses [34–36].

In spite of the considerable body of work available in the literature for the description of molecular alignment both in the impulsive and adiabatic regimes, the experimentalist trying to establish the optimum conditions for aligning a given molecular sample still faces a relative lack of detailed theoretical prediction, especially for intermediate temporal regimes. It is the aim of this paper to contribute to filling this gap and to present a landscape for comparison of laser-induced alignment over a broad range of laser intensities, pulse durations, and temperatures of the sample.

We perform quantum-mechanical calculations on the dynamics of molecular alignment in order to compare directly the degree of alignment achieved with both the adiabatic and the impulsive techniques. We also study the dependence of the degree of alignment on the laser intensity, pulse duration, and temperature of the sample in order to find the optimum alignment conditions. Additionally, we calculate the time-

dependent angular distribution of the impulsively aligned samples in order to provide a more complete description of the alignment dynamics. We limit our study to the alignment in one dimension disregarding the orientation of the molecules. This, however, is enough to fully determine the spatial coordinates of linear molecules with inversion symmetry.

II. MODEL

We consider a linear molecule exposed to a nonresonant linearly polarized laser field

$$\vec{E}(t) = \hat{\epsilon} E_0 f(t) \cos \omega t, \quad (1)$$

where $\hat{\epsilon}$ is a unit vector along the polarization direction, E_0 is the field amplitude, $f(t)$ is the pulse envelope, and ω is the laser frequency. We take the pulse shape to be of the form

$$f(t) = \text{sech}\left(\frac{2 \ln(1 + \sqrt{2})}{\tau} t\right), \quad (2)$$

where τ is the pulse duration (we do not anticipate impulsive alignment to be very sensitive to the pulse shape chosen).

As a consequence of the anisotropy of the molecular polarizability the molecule experiences a potential in the presence of the electric field of the form

$$V_{\text{int}} = -\frac{1}{2} E(t)^2 (\Delta\alpha \cos^2 \theta + \alpha_{\perp}), \quad (3)$$

where $\Delta\alpha$ is the difference between the polarizabilities in the direction parallel and perpendicular to the molecular axis ($\Delta\alpha = \alpha_{\parallel} - \alpha_{\perp}$) also known as “polarizability anisotropy,” α_{\perp} is the polarizability in the direction perpendicular to the molecular axis, and θ is the angle between the molecular axis and the electric field vector.

If the frequency of the laser is much greater than the reciprocal of the laser pulse duration the modulation of the electric field can be averaged giving rise to the following interaction potential:

$$\bar{V}_{\text{int}}/B_0 = -f(t)^2 (\Delta\omega \cos^2 \theta + \omega_{\perp}), \quad (4)$$

where B_0 is the rotational constant in the ground vibrational level, and we have made use of the dimensionless interaction parameters [14]

$$\omega_{\parallel,\perp} \equiv \frac{\alpha_{\parallel,\perp} E_0^2}{4B_0}, \quad (5)$$

$$\Delta\omega \equiv \omega - \omega_{\perp}. \quad (6)$$

Quantum mechanically, the molecule is described as a rigid rotor whose eigenstates, in the absence of the laser field, are labeled with the quantum numbers J and M , and are represented in angular space as the spherical harmonics $Y_J^M(\theta, \phi)$. We also assume that no vibrational levels are populated during the interaction.

Under these nonresonant conditions, the time-dependent interaction potential induces a sequence of Rabi-type cycles each of which is accompanied by the exchange of two quanta

of angular momentum (in a Raman process) between the molecule and the field [24] generating a broad superposition of rotational eigenstates

$$|\psi_{J_i M_i}\rangle = \sum_{J \geq |M_i|} F_{J_i}(t) |JM_i\rangle, \quad (7)$$

where J_i and M_i are the quantum numbers of the initial rotational state (note that $M=M_i$ is conserved in a linearly polarized field). The expansion coefficients $F_{J_i}(t)$ are complex in general and both their phases and moduli vary during the interaction with the laser.

In the adiabatic limit the evolution of the interaction potential is much slower than the time evolution of the relative phases of the wave packet, thus the potential can be considered as static during every infinitesimal time interval. This approximation allows the use of the time-independent Schrödinger equation, whose solutions are the pendular states. However, here, in order to ensure a unified treatment, we will solve the problem dynamically, using the same equations as for the impulsive case.

In contrast the impulsive limit is reached when the variation of the interaction potential is so fast that the relative phases of the wave packet cannot match those of the pendular states for every instantaneous value of the coupling strength. Therefore the superposition of states outlives the laser pulse and the moduli of the components of the wave packet remain constant while the phases keep evolving as they would in a field-free rotor, that is,

$$\phi_J(t) = \phi_J(0) - \frac{E_J t}{\hbar}. \quad (8)$$

E_J are the eigenvalues of the field-free rotor which are given by $E_J = B_0 J(J+1)$ for a rigid rotor. Thus, each component of the wave packet “rotates” with a period defined by J causing a periodic dephasing and rephasing of the wave packet at times multiple of the fundamental rotational period. This leads to the revivals of the aligned state generated in the interaction with the laser pulse.

When the interaction is so strong that high J levels are populated it is necessary to take into account the deformation caused by the centrifugal force in the fast spinning molecules, thus we have to introduce another term in the energy eigenvalues, given by $E_J = B_0 J(J+1) - D_0 J^2(J+1)^2$, where D_0 is the centrifugal distortion parameter. This term breaks the rotational coherence within the wave packet, preventing a perfect reconstruction of the wave packet. It causes a deformation of the revival structures, lowering the maximum degree of alignment and finally deleting all traces of revivals after a number of cycles. Nevertheless, this effect is only relevant in systems at high temperature ($\gamma > 300$) with a strong coupling intensity ($\Delta\omega > 2000$), and usually start to show up after a few rotational cycles. Introducing the state defined by Eq. (7) in the time-dependent Schrödinger equation, the equations for the evolution of the coefficients $F_{J_i}(t)$ are obtained as a set of coupled linear equations

$$\begin{aligned} \frac{i\hbar}{B_0} \dot{F}_{J_i}(t) &= [E_J/B_0 - f(t)^2 \omega_{\perp}] F_{J_i}(t) \\ &\quad - f(t)^2 \Delta\omega \sum_{J'} F_{J_i'}(t) \langle JM | \cos^2 \theta | J'M \rangle \end{aligned} \quad (9)$$

with the initial condition

$$F_{J_i}(0) = \delta_{J_i}(t). \quad (10)$$

Taking into account that the only nonvanishing terms of the summatory are those with $J'=J$ and $J \pm 2$ [23], and using the exact expressions for the matrix elements of $\cos^2 \theta$, Eq. (9) is evaluated numerically using a fourth-order Runge-Kutta algorithm. The impulsively produced wave packets as well as the adiabatic pendular states are thus obtained. The range of initial states considered is set according to the rotational temperature of the sample, also the size of the matrix calculated by Eq. (9) is set in order to span sufficient J space to include the whole rotational wave packet formed in the interaction with the laser.

It is well known that because of the spin statistics of the nuclei, some molecules present only even or odd J states in the electronic ground state, so the abundance of those states depends on the degeneracy of the nuclear spin. The disproportion between even and odd J states causes the appearance of fractional revivals at times multiple of one quarter of the rotational period. For the sake of generality when we refer to the maximum degree of alignment in the impulsive regime, it is calculated at the peak of the full revival, whose appearance is independent of the nuclear spin.

The degree of alignment of a molecular sample is usually defined by the expectation value of $\cos^2 \theta$. When an ensemble of molecules in thermal equilibrium is considered, the expectation value of $\cos^2 \theta$ must be averaged over the Boltzmann distribution of initial rotational states J_i , thus we have [14]

$$\langle\langle \cos^2 \theta \rangle\rangle = \sum_{J_i} w_{J_i} \sum_{M_i=-J_i}^{+J_i} \langle \psi_{J_i M_i} | \cos^2 \theta | \psi_{J_i M_i} \rangle, \quad (11)$$

with $w_{J_i} = \exp[-\gamma J_i(J_i+1)]/Z_r$, where Z_r is the rotational partition function and $\gamma = kT/B_0$ is the reduced rotational temperature. This quantity ranges from 1 for an idealized perfectly aligned sample along the laser polarization axis, to 0 where all the molecules would be delocalized in a plane perpendicular to that axis, and an isotropic sample has $\langle\langle \cos^2 \theta \rangle\rangle = 1/3$.

III. RESULTS AND DISCUSSION

A. Temporal behavior of alignment

The results of the calculations of the time evolution of $\langle\langle \cos^2 \theta \rangle\rangle$ for an ensemble of N_2 molecules at 50 K are depicted in Fig. 1. The molecular parameters used for the calculations in these examples are listed in Table I. The plot in Fig. 1(a) has been obtained with a laser pulse of 50 fs duration and 2.5×10^{13} W/cm² peak intensity. It shows the characteristic features of the impulsive regime, i.e., an enhancement of the alignment after the laser pulse, and the

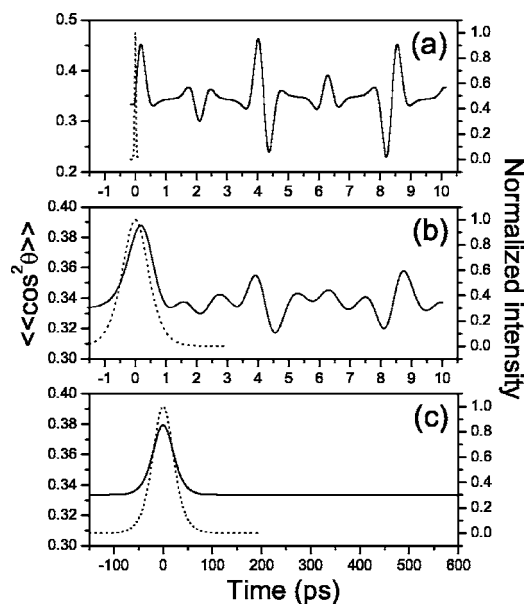


FIG. 1. Time evolution of the degree of alignment in N_2 at 50 K with different pulse durations and peak intensities; (a) $\tau=50$ fs, $I_0=2.5 \times 10^{13}$ W/cm², (b) $\tau=1$ ps, $I_0=2.5 \times 10^{12}$ W/cm², (c) $\tau=50$ ps, $I_0=2.5 \times 10^{12}$ W/cm². The pulse profiles are represented as dotted curves for reference.

appearance of full and half rotational revivals at $t=nT_{\text{rot}}$ and $t=(n+1/2)T_{\text{rot}}$ respectively, where n is an integer number (for N_2 , $T_{\text{rot}}=8.38$ ps). In this case the quarter revivals are also present with half the height of the full and half revivals because there is a disproportion of two to one between even and odd J states in N_2 .

Figure 1(c) shows the time evolution of the degree of alignment in N_2 during a 50-ps-long pulse with a peak intensity of 2.5×10^{12} W/cm², representing the purely adiabatic regime. The maximum degree of alignment in this case is reached at the peak of the laser pulse and after that the ensemble returns smoothly to the isotropic distribution without further realignment.

In Fig. 1(b) an intermediate case is depicted. The maximum degree of alignment is reached during the interaction with the laser pulse like in the purely adiabatic case, but some weak revival structure remains after the pulse. The amplitude of the revivals decreases as the process becomes more adiabatic with longer pulses.

B. Dependence of the degree of alignment in the impulsive regime as a function of the pulse duration

Figure 2 shows the maximum degree of alignment for a generic linear molecule attained in the impulsive regime at

TABLE I. Molecular parameters used in the calculations.

Molecule	$\alpha_{\parallel}(\text{\AA}^3)$	$\alpha_{\perp}(\text{\AA}^3)$	$\Delta\alpha(\text{\AA}^3)$	$B_0(\text{cm}^{-1})$
N_2	2.38 ^a	1.45 ^a	0.93	1.989 ^b
CS_2	15.14 ^a	5.54 ^a	9.6	0.109 ^c

^aFrom Ref. [37].

^bFrom Ref. [38].

^cFrom Ref. [39].

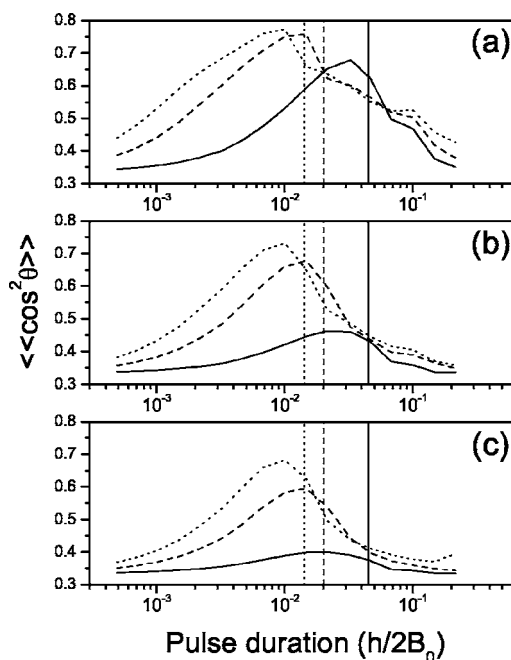


FIG. 2. Maximum degree of alignment at the full revival time as a function of the pulse duration for different temperatures: (a) $\gamma=10$, (b) $\gamma=50$, (c) $\gamma=100$ and coupling strengths: $\Delta\omega=100$ (solid lines), $\Delta\omega=500$ (dashed lines), $\Delta\omega=1000$ (dotted lines). The vertical lines indicate the pulse duration that maximizes the degree of rotational excitation for every value of $\Delta\omega$, calculated with Eq. (12).

the full revival time as a function of the pulse duration (in units of $T_{\text{rot}} \equiv h/2B_0$) for different values of temperature (parametrized by $\gamma=kT/B_0$) and the coupling strength $\Delta\omega$ (note that $\Delta\omega$ is related to the peak intensity of the laser pulse, so that the total energy per pulse increases with the time duration). As the appearance time of the revivals changes with the conditions of the interaction, the full revival has to be tracked, searching the maximum degree of alignment in a time range around T_{rot} , counting from the end of the laser pulse. It can be seen that the value of $\langle\langle \cos^2 \theta \rangle\rangle$ increases with the pulse duration up to a value which maximizes the alignment, and then decreases until there is no alignment at all at the expected revival time.

Considering that the degree of rotational excitation is determined by the competition between the diagonal and off-diagonal terms of Eq. (9), Seidman distinguished two sub-regimes within the impulsive mode [22]: for sufficiently short pulses the degree of rotational excitation (measured as the maximum J state populated from $J_i=0$) depends on the total energy rather than upon the peak intensity of the laser pulse. Thus, for a given intensity, the alignment is limited by the pulse duration. For longer pulses it is determined by the accumulated detuning from resonance and depends exclusively on the laser intensity. The limit between those regimes is set around

$$\tau^2 \Delta\omega \frac{\pi^2}{2} = 1, \quad (12)$$

with τ expressed in units of $h/2B_0$. The first regime takes place for $\tau^2 \Delta\omega (\pi^2/2) \ll 1$ while the second one occurs for

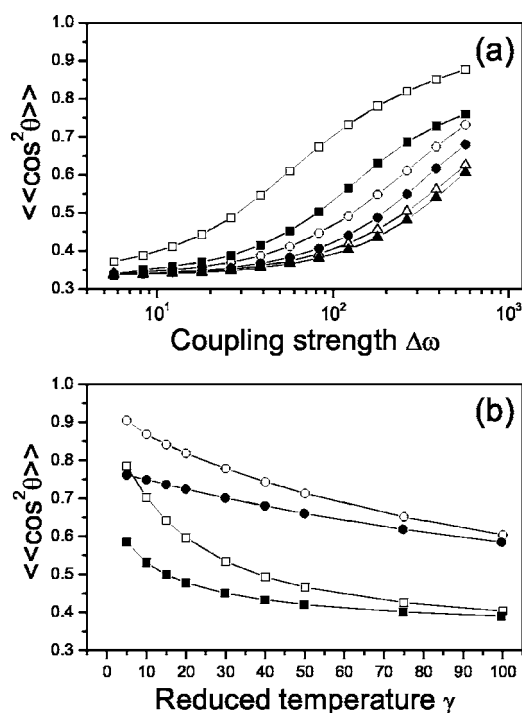


FIG. 3. Maximum degree of alignment attained in the adiabatic regime (open symbols) and impulsive regime with a pulse of $0.01(h/2B_0)$ (solid symbols). (a) As a function of the coupling strength, for $\gamma=10$ (squares), $\gamma=50$ (circles), $\gamma=100$ (triangles). (b) As a function of the reduced temperature for $\Delta\omega=100$ (squares), $\Delta\omega=500$ (circles).

$\tau^2\Delta\omega(\pi^2/2) \gg 1$. The relation given by Eq. (12) thus gives an estimation of the pulse duration that maximizes the degree of rotational excitation for a given intensity and vice versa.

Increasing the pulse duration longer than $(1/\pi)\sqrt{2/\Delta\omega}$ for a fixed $\Delta\omega$ does not change the degree of rotational excitation, which remains at its maximum. The fact that the degree of alignment at the full revival time starts to decrease before reaching the conditions of maximum rotational excitation indicates that the adiabatic behavior starts to take place. This means that the trailing part of the laser pulse begins to cause rotational deexcitation, washing out the revival structure, as can be seen in the transition from Figs. 1(a)–1(c). Therefore, Fig. 2 can be regarded as a visualization of the transition from the impulsive to the adiabatic regimes in terms of the pulse duration.

As we have seen, the maximum degree of alignment achieved when $\tau^2\Delta\omega(\pi^2/2) \ll 1$ depends only on the total energy deposited in the system. This is very advantageous for many applications because it allows the experimenter to have a strongly coupled aligning field while keeping the intensity below the dissociation and ionization thresholds of the molecules.

The optimum pulse duration also depends slightly on temperature, becoming shorter with increasing temperature. This effect is more noticeable with a low coupling strength (solid lines in Fig. 2). The temperature of the sample is known to critically affect the degree of alignment attained in the system because the range of initial rotational levels comprised in the thermal distribution give rise to wave packets without

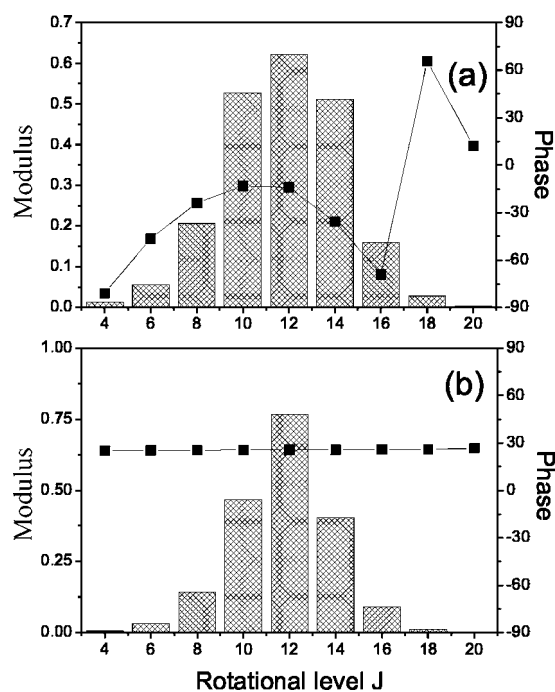


FIG. 4. Rotational wave packets formed in N_2 from the initial state $J_i=12, M_i=0$; (a) after the interaction with a laser pulse of $\tau = 0.01(h/2B_0)$ (83.8 fs) and $\Delta\omega=100$ ($I_0=2 \times 10^{13}$ W/cm 2), at the full revival time; (b) in the interaction with a pulse of $\tau = 3(h/2B_0)$ (25.1 ps) and $\Delta\omega=100$ ($I_0=2 \times 10^{13}$ W/cm 2), at the time of maximum intensity. The bars represent the moduli of the coefficients of the wave packet and the squares represent the phases.

a definite phase relation between them. Therefore, a degree of rotational excitation slightly lower than the maximum achievable, i.e., narrower wave packets, benefits the degree of alignment at high temperatures.

C. Comparison between adiabatic and impulsive alignment

Figure 3 shows the dependence of the peak value of $\langle\langle \cos^2 \theta \rangle\rangle$ in a molecular ensemble on the laser intensity and rotational temperatures for both the adiabatic and impulsive regimes. The pulse duration for the latter case has been chosen to be $0.01(h/2B_0)$, that is around the optimum found in the last section. In both cases the degree of alignment decreases with temperature and increases with the laser intensity as expected [14,22,29], the limit for the intensity being the threshold of dissociation or ionization of the molecules.

It can be seen that at low intensities the degree of alignment reached in the adiabatic regime is much higher than in the impulsive case at the same laser intensity and temperature conditions. As seen in the previous section, the rotational excitation is maximum when the condition defined by Eq. (12) is fulfilled, so the long pulses used in the adiabatic regime do not produce a higher degree of rotational excitation. The reason why the degree of alignment is better in the adiabatic than in the impulsive regime at the same conditions must be found in the relative phases within the wave packets. While all the rotational components of a pendular state have

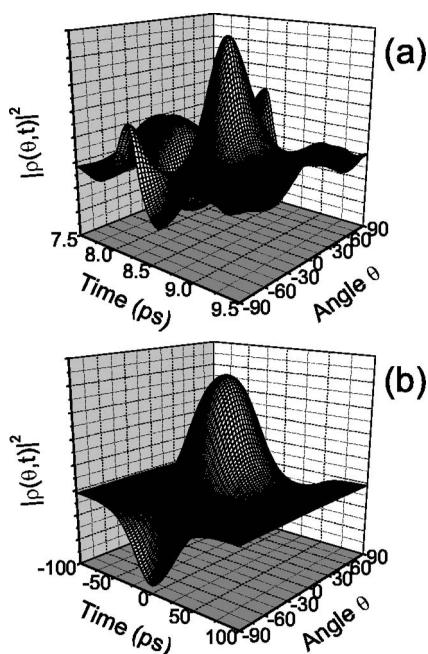


FIG. 5. Angular distribution of an ensemble of N_2 at 50 K. (a) Around the full revival time after the interaction with a laser pulse of 50 fs duration and $I_0=2.5 \times 10^{13}$ W/cm 2 peak intensity. (b) During the interaction with a 50 ps and $I_0=2.5 \times 10^{12}$ W/cm 2 laser pulse.

the same phase, in the impulsively produced wave packets each component has a different phase even at the time of the revival peak (see Fig. 4).

The full revival peak is known to reproduce the wave packet at the time of maximum alignment immediately after the intensity peak of the laser pulse, but the components of this wave packet are not necessarily in phase. During the interaction, as the laser excitation adds new components to the wave packet, the corresponding phases evolve in such a manner that all of them tend to get the same phase. The phase matching can be completed with the long pulses used in the adiabatic technique, but in the impulsive regime the short pulse vanishes before achieving a complete phase matching, especially at high temperatures as the high J levels involved in that case have more inertia. The maximum degree of alignment is thus attained some time after the intensity peak of the laser pulse, when the field-free evolution of the wave packet eventually produces a state of minimum phase dispersion.

Notwithstanding the lower degrees of alignment achieved in the impulsive technique as compared to the adiabatic for the same conditions, it must be pointed out that the peak intensities accessed by the short laser pulses required for the impulsive methods can exceed by a large factor those reached by the relatively long pulses used in the adiabatic case. In fact, the intensities used typically in the experiments with impulsive alignment range between 10^{13} – 10^{14} W/cm 2 [30,32,33] while in the adiabatic experiments they are usually lower than 2×10^{12} W/cm 2 [11,16]. Thus, in practice, the degrees of alignment achieved in the laboratory with the impulsive technique may be similar or even higher than the adiabatic ones.

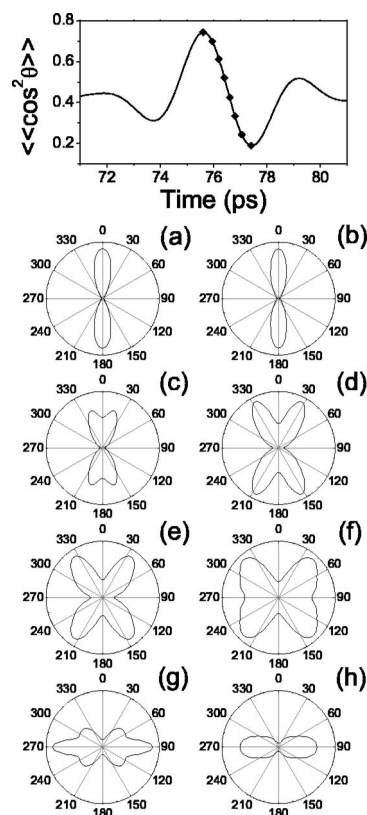


FIG. 6. Snapshots of the angular distribution of an ensemble of CS_2 at 10 K aligned by a laser pulse of 10^{13} W/cm 2 and 100 fs duration, around a full revival; (a) $t=75.60$ ps, (b) $t=75.95$ ps, (c) $t=76.20$ ps, (d) $t=76.40$ ps, (e) $t=76.60$ ps, (f) $t=76.80$ ps, (g) $t=77.05$ ps, (h) $t=77.40$ ps. The inset shows the points in the $\langle\langle\cos^2\theta\rangle\rangle$ plot corresponding to each snapshot. The radii are not at the same scale.

D. Angular distribution in the impulsive regime

The impulsive technique has the feature of producing field-free aligned distributions that change rapidly with time. In order to provide a more complete description of the alignment dynamics in the short-pulse regime, we have calculated the time-dependent angular distributions of the molecular ensemble as the thermal average of the squared modulus of the rotational wave packets

$$|\rho(\theta,t)|^2 = \sum_{J_i} w_{J_i} \sum_J \sum_{J'} F_{J,J} F_{J,J'}^* Y_J^M(\theta) Y_{J'}^M(\theta), \quad (13)$$

where w_{J_i} are the thermal coefficients defined elsewhere, $F_{J,J}$ are the coefficients defined by Eq. (9), $F_{J,J'}^*$ are the complex conjugates, and $Y_J^M(\theta)$ are the projection of the spherical harmonics onto the plane $\phi=0$. Note that the full 3D distribution must include the factor $\sin\theta$ which accounts for the weighting over the azimuthal angle ϕ .

Figure 5(a) shows the angular distribution of an ensemble of impulsively aligned N_2 at 50 K, around a revival peak. As a contrast, the distribution formed during the interaction with a 50-ps-long pulse is shown in Fig. 5(b). The distribution formed after the short pulse interaction presents the expected maxima around 0° and $\pm 90^\circ$ which can be inferred from the

$\langle\langle \cos^2 \theta \rangle\rangle$ plots, but also provides some additional information. Angular distribution measurements from impulsively aligned samples have shown a structured angular distribution at times where there are no revivals in the $\langle\langle \cos^2 \theta \rangle\rangle$ plot [30]. These distributions give similar values of $\langle\langle \cos^2 \theta \rangle\rangle$ than the isotropic ones. However, an angular distribution showing some degree of order can be very relevant in strong-field processes with molecules.

It is particularly important to determine whether the transition from the aligned to the antialigned distribution (or vice versa) during a revival passes through an isotropic distribution or rather through a series of aligned distributions at intermediate angles. Figure 6 shows different snapshots of the angular distribution from the maximum to the minimum of $\langle\langle \cos^2 \theta \rangle\rangle$ inside a revival of CS₂ at 10 K. Between the aligned and antialigned distributions, the ensemble deploys a rich variety of butterfly-shaped distributions, presenting always some degree of order, with the most probable alignment angles varying around 30° as it evolves in time inside the revival.

The appearance of butterfly-shaped distributions is independent of the molecule and the conditions of the interaction. It has been reported recently that both the probability of ionization and the harmonic yield from a given molecule are dependent on the angle between the molecular axis and the driving field polarization in accordance to the geometry of the HOMO [3,4,6–12]. In fact, it has been possible to observe the occurrence of rotational revivals in impulsive aligned molecules in terms of harmonics and ion signal [40–42]. The shape of the revivals in ion yield or harmonic signal is determined by the angle that maximizes both processes, and a correlation between those measurements and the angular distribution of the molecular sample can thus be established.

IV. CONCLUSIONS

We have examined the dynamics of strong field nonresonant laser-induced alignment of linear molecules. The main results of this work are (i) the demonstration that for the same laser intensity the adiabatic limit leads to higher degrees of alignment than in the impulsive limit, (ii) the dependence of the peak alignment upon laser pulse duration is examined and explained, and (iii) the detailed evolution of the molecular ensemble angular distribution during the central part of an alignment revival is explicitly evaluated. The results are obtained for a generic linear molecule and so are generally relevant to any appropriate diatomic or triatomic molecular system (e.g., N₂, O₂, I₂, CO₂). These results enable us to better understand the behavior of molecules in real experiments. The basis for comparison not only between the impulsive and adiabatic limit but for intermediate pulse duration has been explored. This is potentially important as for a number of implementations of alignment laser pulses stretched to durations in the ~100 fs–few ps regime (intermediate) are often used. Also knowledge of details of the angular distribution of the ensemble as it evolves through a revival is important for future experiments where probes much shorter than the duration of the revival are used.

ACKNOWLEDGMENTS

We thank Jonathan Underwood and Raffaele Velotta for fruitful discussions. R. T. acknowledges the Spanish Ministry for Education and Science for financial support. R. N. also acknowledges the Spanish Ministry for Education and Science and Universidad Complutense de Madrid for a Ramon y Cajal research contract. This work has been supported by the RCUK and EPSRC and the EU.

-
- [1] J. Muth-Böhm, A. Becker, and F. H. M. Faisal, *Phys. Rev. Lett.* **85**, 2280 (2000).
- [2] M. Lein, *J. Phys. B* **36**, L155 (2003).
- [3] I. V. Litvinyuk, K. F. Lee, P. W. Dooley, D. M. Rayner, D. M. Villeneuve, and P. B. Corkum, *Phys. Rev. Lett.* **90**, 233003 (2003).
- [4] A. Jaron-Becker, A. Becker, and F. H. M. Faisal, *Phys. Rev. A* **69**, 023410 (2004).
- [5] B. Shan, S. Ghimire, and Z. Chang, *Phys. Rev. A* **69**, 021404(R) (2004).
- [6] R. de Nalda, E. Heesel, M. Lein, N. Hay, R. Velotta, E. Sprin-gate, M. Castillejo, and J. P. Marangos, *Phys. Rev. A* **69**, 031804(R) (2004).
- [7] D. G. Lappas and J. P. Marangos, *J. Phys. B* **33**, 4679 (2002).
- [8] R. Velotta, N. Hay, M. B. Mason, M. Castillejo, and J. P. Marangos, *Phys. Rev. Lett.* **87**, 183901 (2001).
- [9] M. Lein, N. Hay, R. Velotta, J. P. Marangos, and P. L. Knight, *Phys. Rev. Lett.* **88**, 183903 (2002).
- [10] M. Lein, N. Hay, R. Velotta, J. P. Marangos, and P. L. Knight, *Phys. Rev. A* **66**, 023805 (2002).
- [11] N. Hay, R. Velotta, M. Lein, R. de Nalda, E. Heesel, M. Castillejo, and J. P. Marangos, *Phys. Rev. A* **65**, 053805 (2002).
- [12] M. Lein, P. P. Corso, J. P. Marangos, and P. L. Knight, *Phys. Rev. A* **67**, 023819 (2003).
- [13] J. Itatani, J. Levesque, D. Zeidler, H. Niikura, H. Pepin, J. C. Kieffer, P. B. Corkum, and D. M. Villeneuve, *Nature (London)* **432**, 867 (2004).
- [14] B. Friedrich and D. Herschbach, *Phys. Rev. Lett.* **74**, 4623 (1995).
- [15] B. Friedrich and D. Herschbach, *J. Phys. Chem.* **99**, 15686 (1995).
- [16] J. J. Larsen, H. Sakai, C. P. Safvan, I. Wendt-Larsen, and H. Stapelfeldt, *J. Chem. Phys.* **111**, 7774 (1999).
- [17] T. Seideman, *J. Chem. Phys.* **103**, 7887 (1995).
- [18] H. Stapelfeldt and T. Seideman, *Rev. Mod. Phys.* **75**, 543 (2003).
- [19] H. J. Loesch and A. Remscheid, *J. Chem. Phys.* **93**, 4779 (1990).
- [20] M. Wu, R. J. Bemish, and R. E. Miller, *J. Chem. Phys.* **101**, 9447 (1994).
- [21] Even if the molecule has a permanent dipole moment, its in-

- teraction with the electric field is averaged to zero over a laser pulse when the frequency is much greater than the inverse of the pulse duration.
- [22] T. Seideman, *J. Chem. Phys.* **115**, 5965 (2001).
- [23] J. Ortigoso, M. Rodriguez, M. Gupta, and B. Friedrich, *J. Chem. Phys.* **110**, 3870 (1999).
- [24] T. Seideman, *Phys. Rev. Lett.* **83**, 4971 (1999).
- [25] R. A. Bartels, T. C. Weinacht, N. Wagner, M. Baertschy, C. H. Greene, M. M. Murnane, and H. C. Kapteyn, *Phys. Rev. Lett.* **88**, 013903 (2002).
- [26] M. Comstock, V. V. Lozoyov, and M. Dantus, *Chem. Phys. Lett.* **372**, 739 (2003).
- [27] J. G. Underwood, B. J. Sussman, and A. Stolow, *Phys. Rev. Lett.* **94**, 143002 (2005).
- [28] Z.-C. Yan and T. Seideman, *J. Chem. Phys.* **111**, 4113 (1999).
- [29] F. Rosca-Pruna and M. J. J. Vrakking, *J. Chem. Phys.* **116**, 6579 (2002).
- [30] P. W. Dooley, I. V. Litvinyuk, K. F. Lee, D. M. Rayner, M. Spanner, D. M. Villeneuve, and P. B. Corkum, *Phys. Rev. A* **68**, 023406 (2003).
- [31] E. Peronne, M. D. Poulsen, C. Z. Bisgaard, H. Stapelfeldt, and T. Seideman, *Phys. Rev. Lett.* **91**, 043003 (2003).
- [32] V. Renard, M. Renard, S. Guerin, Y. T. Pashayan, B. Lavorel, O. Faucher, and H. R. Jauslin, *Phys. Rev. Lett.* **90**, 153601 (2003).
- [33] F. Rosca-Pruna and M. J. J. Vrakking, *J. Chem. Phys.* **116**, 6567 (2002).
- [34] I. Sh. Averbukh and R. Arvieu, *Phys. Rev. Lett.* **87**, 163601 (2001).
- [35] C. M. Dion, A. B. Haj-Yedder, E. Cances, C. Le Bris, A. Keller, and O. Atabek, *Phys. Rev. A* **65**, 063408 (2002).
- [36] M. Leibscher, I. Sh. Averbukh, and H. Rabitz, *Phys. Rev. Lett.* **90**, 213001 (2003).
- [37] J. O. Hirschfelder, C. F. Curtiss, and R. B. Bird, *Molecular Theory of Gases and Liquids* (Wiley, New York, 1954).
- [38] K. P. Huber and G. Herzberg, *NIST Chemistry WebBook*, edited by P. J. Linstrom and W. G. Mallard (National Institute of Standards and Technology, Gaithersburg, MD, 2001).
- [39] A. M. James and M. P. Lord, *MacMillan's Chemical and Physical Data* (MacMillan, London, 1992).
- [40] M. Kaku, K. Masuda, and K. Miyazaki, *Jpn. J. Appl. Phys., Part 2* **43**, L591 (2004).
- [41] J. Itatani, D. Zeidler, J. Levesque, M. Spanner, D. M. Villeneuve, and P. B. Corkum, *Phys. Rev. Lett.* **94**, 123902 (2005).
- [42] T. Kanai, S. Minemoto, and H. Sakai, *Nature (London)* **435**, 470 (2005).